Thermodynamics and Kinetics of Nucleation

Lecturer: Prof Ian Ford, Department of Physics and Astronomy, UCL

Contents

1 Introduction **2**

2 Density fluctuations in an ideal gas **2**

3 Nonideal gases and the virial expansion **3**
3.1 Two particle system . . . 3
3.2 Many particle fluid . . . 4
3.3 Weakly attractive hard sphere fluid to lowest order approximation . . . 5
3.4 Carnahan-Starling model of weakly attractive hard sphere fluid . . . 6

4 Phase coexistence **7**
4.1 The availability potential . . . 7
4.2 Availability of a weakly attractive hard sphere fluid . . . 8

5 Density fluctuations in a nonideal gas **9**

6 Cluster dynamics and droplet nucleation **11**
6.1 Becker-Döring equations . . . 11
6.2 Nucleation barrier and critical size . . . 12
6.3 Solution to the rate equations . . . 13
6.4 Classical nucleation theory . . . 16

7 Nucleation and the second law **18**

1 Introduction

In these notes we seek to understand how it is that phases of materials, such as gases and liquids, can coexist, and to identify the way in which they transform into one another and the rate at which they do so. Most common phase transitions occur by virtue of the phenomenon known as *nucleation*, where a tiny fragment of the new phase grows out of the old phase, initially impeded by the need to surmount a thermodynamic barrier. The existence of such a barrier makes it possible to maintain the old phase in a state of metastability for some considerable time, for example water can be kept in its liquid phase at temperatures as low as -40° C at room pressure, if one is careful, even though its phase diagram would require it to turn into ice. Sections 2-5 of these notes address the statistical mechanics of coexistence between the gas and liquid phases of a weakly attractive hard sphere fluid, and the remaining sections are concerned with the kinetics of a nucleated phase transition: the rate of crossing of the barrier. In these later sections we shall proceed in a general framework, but the approximate classical theory of nucleation will be introduced to illustrate some points. Finally, we consider the nonequilibrium thermodynamics of the process of nucleation and consider whether it is compatible with the second law.

2 Density fluctuations in an ideal gas

The ideal gas is a system where analytic treatment of the equilibrium statistical mechanics is possible. The canonical partition function of an ideal gas of N spin zero particles of mass m in three dimensions is easy to compute:

$$Z_N^{\rm ig} = \frac{1}{h^{3N}N!}\int \prod_{i=1}^{N} {\rm d}\boldsymbol{p}_i {\rm d}\boldsymbol{x}_i \ \exp[-\sum_{i=1}^{N} \boldsymbol{p}_i^2/(2mkT)] = \frac{1}{N!}\prod_{i=1}^{N}\int \frac{1}{\lambda_{\rm th}^3}{\rm d}\boldsymbol{x}_i = \frac{(Vn_q)^N}{N!}, \qquad (1)$$

where $n_q(T) = (2\pi mkT/h^2)^{3/2}$ is the quantum concentration, equal to the inverse of the cube of the thermal de Broglie wavelength $\lambda_{\rm th}$. The quantum concentration is not only the threshold spatial density of a gas above which it exhibits quantum effects, but it also acts as if it were a density of microstates in three dimensional coordinate space. The thermal de Broglie wavelength is the effective spatial separation between microstates in such a phase space. Note that the indistinguishability correction appears here since the classical dynamics allow particles to swap positions. The correction is an approximate way to recognise that this should not be treated as a distinct configuration, as a consequence of the dictates of quantum mechanics.

The Helmholtz free energy for large N is $F_{\rm ig} = -kT\ln Z_N^{\rm ig} \approx -kT[N\ln(Vn_q) - N\ln N + N] = NkT[\ln(n/n_q)-1]$, with particle density $n = N/V$, having used Stirling's approximation. Notice that the indistinguishability correction makes F extensive, as required. The grand canonical partition function for chemical potential μ is:

$$Z_G(\mu,V,T) = \sum_{N=0}^{\infty}\exp(\mu N/kT)Z_N^{\rm ig} = \sum_{N=0}^{\infty}\frac{[Vn_q\exp(\mu/kT)]^N}{N!} = \exp[Vn_q\exp(\mu/kT)], \qquad (2)$$

and we can then identify the grand potential $\Phi(\mu,V,T) = -kT\ln Z_G = -kTVn_q\exp(\mu/kT)$. We can then compute, using the method of the grand canonical ensemble, the mean number of particles found in volume V when the chemical potential of the gas is μ:

$$\langle N\rangle = \frac{1}{Z_G}\sum_{N=0}^{\infty} N \ \exp(\mu N/kT)Z_N^{\rm ig} = kT\left(\frac{\partial \ln Z_G}{\partial\mu}\right)_{V,T} = Vn_q\exp(\mu/kT) = \ln Z_G. \qquad (3)$$

This can be inverted to relate the chemical potential of the reservoir to the mean population in the system:

$$\mu = kT\ln[\langle N\rangle/(n_qV)], \qquad (4)$$

becoming $\mu \approx kT\ln(n/n_q)$ for a large system with negligible population fluctuations. If a gas exceeds the quantum concentration it begins to exhibit quantum properties, so that the chemical potential of a *classical* ideal gas is negative since $\langle N\rangle/V \ll n_q$. In order to increase the mean population in the system, we need to increase μ, meaning that it should become less negative.

Similarly, the mean square population in the system for the ideal classical gas is

$$\langle N^2\rangle = \frac{1}{Z_G}\sum_{N=0}^{\infty} N^2 \ \exp(\mu N/kT)Z_{\rm ig} = \frac{(kT)^2}{Z_G}\left(\frac{\partial^2 Z_G}{\partial\mu^2}\right)_{V,T}, \qquad (5)$$

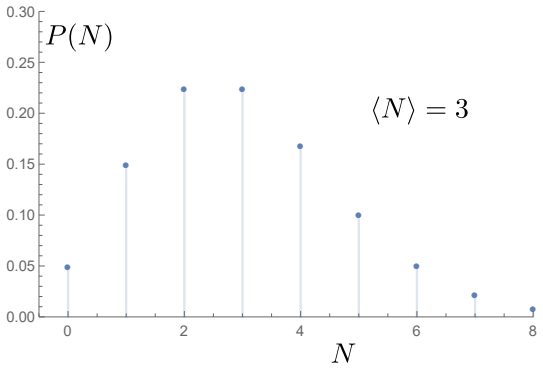

Figure 1: Probability distribution of the number of non-interacting particles N in a system that is in contact with a heat and particle bath at a given temperature and chemical potential. The mean population, given by Eq. (3), is equal to three for the chosen system volume.

reducing to

$$\begin{aligned}\langle N^2\rangle &= \frac{kT}{Z_G}\frac{\partial}{\partial\mu}Z_G\langle N\rangle = \frac{kT}{Z_G}\frac{\partial}{\partial\mu}Z_G\ln Z_G \\ &= kT\frac{\partial}{\partial\mu}\ln Z_G + kT\ln Z_G\frac{\partial}{\partial\mu}\ln Z_G = \ln Z_G + (\ln Z_G)^2,\end{aligned} \tag{6}$$

so

$$\langle N^2\rangle = (1+\langle N\rangle)\langle N\rangle, \tag{7}$$

which nicely illustrates the typical observation in equilibrium systems that the variance in population $\sigma^2 = \langle N^2\rangle - \langle N\rangle^2$ is proportional to the mean.

Density fluctuations in an ideal gas will only be appreciable when we consider a system volume such that the mean population is small. For example, if the mean is 10^{12} particles (for an ideal gas at room pressure and temperature this would require the system volume to be a cube of side 0.1 mm), then the standard deviation would be 10^6 or one millionth of the mean. In contrast, if the sides of the cube were of order 10 nm, the mean and standard deviation of the population would be about 10 and 3, respectively. It is at the nanoscale, well away from the thermodynamic limit, that the detailed canonical statistics (not just the expectation values) prove to be important.

A further conclusion we can reach from this analysis of the classical ideal gas in equilibrium is that the probability that a volume V should contain N particles is

$$P(N) = \frac{1}{Z_G}\exp(\mu N/kT)Z_N^{\text{ig}} = \frac{1}{Z_G}\frac{[Vn_q\exp(\mu/kT)]^N}{N!} = \frac{1}{N!}\langle N\rangle^N\exp(-\langle N\rangle), \tag{8}$$

having inserted $\ln Z_G = \langle N\rangle$. This is a Poisson distribution, illustrated in Figure 1, that describes the likelihood of the occurrence of N independent events (that we might visualise in this case as particle insertions into the system volume from the surrounding gas). Later on we shall study how this distribution is modified and can become *bimodal* when interactions between the particles are introduced. We'll also explore how an arbitrary distribution might evolve in time towards such a stationary form, through the process of *nucleation*.

3 Nonideal gases and the virial expansion

We study *nonideal* gases in order to compute the free energy of a set of interacting particles. It will be apparent that approximations now have to be made. We shall restrict our discussion to particles with zero spin.

3.1 Two particle system

We start with a system of two particles of equal mass that interact through a potential $\phi(r_{12})$ where r_{12} is their separation. The Hamiltonian is $H(\boldsymbol{p}_1,\boldsymbol{p}_2,\boldsymbol{x}_1,\boldsymbol{x}_2) = |\boldsymbol{p}_1|^2/(2m)+|\boldsymbol{p}_2|^2/(2m)+\phi(|\boldsymbol{x}_1-\boldsymbol{x}_2|)$

and the canonical partition function is

$$Z_2 = \frac{1}{h^6 2!} \int \prod_{i=1}^{2} \mathrm{d}^3\boldsymbol{p}_i \mathrm{d}^3\boldsymbol{x}_i \, \exp(-H/kT). \tag{9}$$

The integration is to be performed over all values of momenta, and all particle positions within a (large) box of volume V. We transform to spatial coordinates $\boldsymbol{R} = \frac{1}{2}(\boldsymbol{x}_1 + \boldsymbol{x}_2)$ and $\boldsymbol{r}_{12} = \boldsymbol{x}_1 - \boldsymbol{x}_2$, with a Jacobian of unity, and perform the momentum integrals to get

$$Z_2 = \frac{1}{2}\left(\frac{2\pi mkT}{h^2}\right)^3 \int \mathrm{d}^3\boldsymbol{R}\,\mathrm{d}^3\boldsymbol{r}_{12} \, \exp(-\phi(r_{12})/kT) = \frac{1}{2}V^2 n_q^2 \alpha, \tag{10}$$

where $n_q = (2\pi mkT/h^2)^{3/2}$ is once again the quantum concentration. We have defined

$$\alpha = \frac{1}{V}\int_0^\infty 4\pi r_{12}^2 \exp(-\phi(r_{12})/kT)\mathrm{d}r_{12}, \tag{11}$$

having assuming the integral converges. α would be unity if the interaction potential were zero, but otherwise it expresses the deviation from the behaviour of two noninteracting classical particles (an $N = 2$ ideal gas), which would be represented by a partition function $Z_2^{\mathrm{ig}} = \frac{1}{2}(n_q V)^2 = \frac{1}{2}(Z_1^{\mathrm{ig}})^2$.

It is convenient to write

$$\alpha = 1 + \frac{1}{V}\int_0^\infty 4\pi r^2 f(r,T)\mathrm{d}r = 1 + \frac{\mathcal{B}(T)}{V}, \tag{12}$$

in terms of a temperature dependent quantity $\mathcal{B}(T)$

$$\mathcal{B}(T) = \int_0^\infty 4\pi r^2 f(r,T)\mathrm{d}r, \tag{13}$$

where

$$f(r,T) = \exp(-\phi(r)/kT) - 1, \tag{14}$$

is called the Mayer function, such that

$$Z_2 = \frac{1}{2}V^2 n_q^2(T)\left(1 + \frac{\mathcal{B}(T)}{V}\right) = Z_2^{\mathrm{ig}}\left(1 + \frac{\mathcal{B}(T)}{V}\right), \tag{15}$$

from which thermodynamic properties follow. For example, the pressure is

$$p = kT\left(\frac{\partial \ln Z_2}{\partial V}\right)_T = kT\left(\frac{\partial \ln Z_2^{\mathrm{ig}}}{\partial V}\right)_T + kT\left(\frac{\partial \ln(1+\mathcal{B}/V)}{\partial V}\right)_T = \frac{2kT}{V} - kT\left(1+\frac{\mathcal{B}}{V}\right)^{-1}\frac{\mathcal{B}}{V^2}, \tag{16}$$

and we can regard the second term as a nonideal correction to the ideal gas pressure expressed by the first term.

3.2 Many particle fluid

The procedure can be extended to a gas of N particles in a box. The partition function is now

$$\begin{aligned}
Z_N &= \frac{1}{N!}n_q^N \int \prod_{i=1}^{N} \mathrm{d}^3\boldsymbol{x}_i \, \exp(-\sum_{j>i}\phi(r_{ij})/kT) = \frac{1}{N!}n_q^N \int \prod_{i=1}^{N} \mathrm{d}^3\boldsymbol{x}_i \prod_{j>i}(\exp(-\phi(r_{ij})/kT)) \\
&= \frac{1}{N!}n_q^N \int \prod_{i=1}^{N} \mathrm{d}^3\boldsymbol{x}_i \prod_{j>i}(1+f(r_{ij},T)) = \frac{1}{N!}n_q^N \int \prod_{i=1}^{N} \mathrm{d}^3\boldsymbol{x}_i \, (1+f(r_{12},T))\,(1+f(r_{13},T))\cdots \\
&\approx \frac{1}{N!}n_q^N \left(V^N + \frac{N(N-1)}{2}\int \prod_{i=3}^{N} \mathrm{d}^3\boldsymbol{x}_i \mathrm{d}^3\boldsymbol{x}_1 \mathrm{d}^3\boldsymbol{x}_2 \, f(r_{12},T)\right) + \text{terms in } f^2 \\
&= \frac{1}{N!}(Vn_q)^N \left(1 + \frac{N(N-1)}{2V^2}\int \mathrm{d}^3\boldsymbol{x}_1 \mathrm{d}^3\boldsymbol{x}_2 \,(\exp(-\phi(r_{12})/kT) - 1)\right),
\end{aligned} \tag{17}$$

where r_{ij} is the distance between particles i and j. Notice that on the third line only contributions to the integrand involving a single f function have been retained, and it has been recognised that

there are $\frac{1}{2}N(N-1)$ of them corresponding to the number of particle pairs. Volume integrations have been performed where possible. It will turn out that the Mayer approach corresponds to an expansion in the particle density N/V, also known as a virial expansion.

We write $\mathrm{d}^3\boldsymbol{x}_1\mathrm{d}^3\boldsymbol{x}_2 = \mathrm{d}^3\boldsymbol{R}\,\mathrm{d}^3\boldsymbol{r}_{12} = \mathrm{d}^3\boldsymbol{R}\,4\pi r_{12}^2\mathrm{d}r_{12}$ and use Eqs. (1) and (12) to give

$$Z_N \approx Z_N^{\mathrm{ig}}\left(1 + \frac{N(N-1)}{2V}\mathcal{B}\right), \tag{18}$$

which is consistent with Eq. (15) for $N = 2$, and then we can obtain the pressure

$$p = kT\left(\frac{\partial \ln Z_N}{\partial V}\right)_{T,N} \approx \frac{NkT}{V} - kT\left(1 + \frac{N(N-1)}{2V}\mathcal{B}\right)^{-1}\frac{N(N-1)\mathcal{B}}{2V^2} \approx nkT - \frac{1}{2}kT\mathcal{B}n^2. \tag{19}$$

We have expressed the result in terms of $n = N/V$ and assumed $N \gg 1$. We take $N^2\mathcal{B}/V$ to be small compared with unity and have neglected terms proportional to n^3 and beyond.

It is apparent that we have derived a microscopic form for the so-called second virial coefficient:

$$B_2(T) = -\tfrac{1}{2}\mathcal{B} = \int_0^\infty 2\pi r^2\left(1 - \exp(-\phi(r)/kT)\right)\mathrm{d}r, \tag{20}$$

that appears in the *virial equation of state* of a nonideal gas:

$$\frac{p}{kT} = \sum_{i=1}^{\infty} B_i(T)n^i. \tag{21}$$

The properties of a nonideal gas can be understood by computing as many virial coefficients as possible, in order to describe an increasingly dense gas.

3.3 Weakly attractive hard sphere fluid to lowest order approximation

As an example, consider a *weakly attractive hard sphere* interaction potential where $\phi(r)$ is equal to infinity for $r < r_{\mathrm{p}}$, corresponding to a rigid repulsion at that particle separation (the hard sphere diameter), but small in magnitude in comparison with kT for $r \geq r_{\mathrm{p}}$, as illustrated in Figure 2. We can write

$$\begin{aligned} B_2(T) &= \frac{2\pi}{3}r_{\mathrm{p}}^3 + \int_{r_{\mathrm{p}}}^\infty 2\pi r^2\left(1 - \exp(-\phi(r)/kT)\right)\mathrm{d}r \\ &\approx \frac{2\pi}{3}r_{\mathrm{p}}^3 + \int_{r_{\mathrm{p}}}^\infty 2\pi r^2\frac{\phi(r)}{kT}\mathrm{d}r = b - \frac{a}{kT}, \end{aligned} \tag{22}$$

with positive coefficients

$$b = 2\pi r_{\mathrm{p}}^3/3 \qquad \text{and} \qquad a = -\int_{r_{\mathrm{p}}}^\infty 2\pi r^2\phi(r)\mathrm{d}r. \tag{23}$$

We have introduced notation that allows the derived approximate equation of state to be related to the framework introduced by van der Waals $(p + an^2)(1 - bn) = nkT$, which can be written

$$\left(p + an^2\right) = nkT(1 - bn)^{-1} \approx nkT(1 + bn) \quad \Rightarrow \quad \frac{p}{kT} \approx n\left(1 + \left(b - \frac{a}{kT}\right)n + O(n^2)\right), \tag{24}$$

in a virial form. Thus the b parameter in the van der Waals equation of state is of the order of the particle volume and a is a measure of the mutual interaction energy of a particle pair. If ϕ took a different form, such as the Lennard-Jones expression also shown in Figure 2, or if $\phi(r)$ were not much smaller than kT, the second virial coefficient would have a more elaborate temperature dependence and bear a more complicated relationship to the strength and range of the interaction.

Returning to the case of weakly attractive hard spheres we have, starting from Eq. (18),

$$Z_N \approx Z_N^{\mathrm{ig}}\left(1 - nNB_2\right) = Z_N^{\mathrm{ig}}\left(1 - nN\left(b - \frac{a}{kT}\right)\right). \tag{25}$$

The mean energy of the gas per unit volume $e = \langle E\rangle/V$ follows from $\langle E\rangle = -\mathrm{d}\ln Z_N/\mathrm{d}\beta$, namely

$$e(n,T) \approx \tfrac{3}{2}nkT - n^2kT^2\frac{\mathrm{d}B_2(T)}{\mathrm{d}T} \approx \tfrac{3}{2}nkT + n^2\int_{r_{\mathrm{p}}}^\infty 2\pi r^2\phi(r)\mathrm{d}r. \tag{26}$$

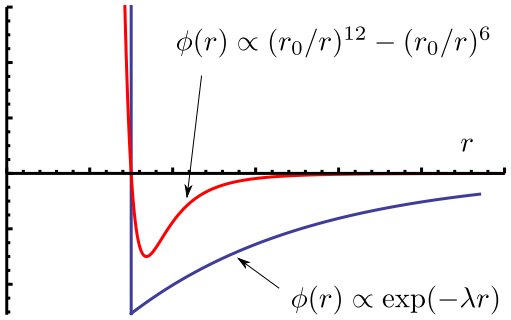

Figure 2: Two commonly chosen interaction pair potentials: in red the so-called Lennard-Jones 6-12 potential with range parameter r_0, and in blue a potential that is exponentially attractive, specified by parameter λ, with a hard repulsion at a minimum separation.

The nonideal term is clearly a mean potential energy that supplements the mean kinetic energy of the first term. The dependence on n^2 arises since we are considering a pairwise interaction and therefore the additional energy should be proportional to the number of particle pairs in the system, which goes as n^2.

The entropy of the gas follows from the identity $S = -(\partial F/\partial T)_{V,N}$ with Helmholtz free energy $F = -kT \ln Z_N$, namely

$$S = S_{\rm ig} - \frac{N^2 k}{V} \frac{{\rm d}(TB_2(T))}{{\rm d}T} = S_{\rm ig} - nkNb = S_{\rm ig} + \Delta S_{\rm AHS}, \tag{27}$$

suggesting that the interactions reduce the entropy of the gas, per particle, by an amount (in this approximation) proportional to the volume Nb that each particle is unable to explore in the system as a consequence of the interparticle repulsion.

The free energy of the system of attractive hard spheres is obtained from Eq. (25):

$$\begin{aligned} F_{\rm AHS} &= -kT \ln Z_N \approx -kT \ln Z_N^{\rm ig} - kT \ln \left(1 - nN\left(b - \frac{a}{kT}\right)\right) \\ &\approx F_{\rm ig} + kTnN\left(b - \frac{a}{kT}\right) = F_{\rm ig} + \Delta E_{\rm AHS} - T\Delta S_{\rm AHS}, \end{aligned} \tag{28}$$

where $\Delta E_{\rm AHS} = -nNa$ and $\Delta S_{\rm AHS} = -nkNb$ represent the changes in entropy and energy with respect to the ideal gas brought about by the attractive hard sphere interactions (to this level of approximation, the change in entropy is only brought about by the repulsions and not the attractions, and the other way round for the change in energy). $\Delta E_{\rm AHS}$ is a sum of mean cohesive energies $-na$ per particle.

By including more terms in the partition function, beyond the cutoff made in Eq. (17), further contributions to the pressure, energy and entropy of the gas can be obtained, corresponding to higher virial coefficients. They rapidly become rather complicated to compute, but they can in principle all be obtained from a specification of the microscopic interactions.

3.4 Carnahan-Starling model of weakly attractive hard sphere fluid

For hard spheres without long range interactions, i.e. the model considered previously but with $\phi = 0$ for $r > r_{\rm p}$, it has been shown that the next few terms in the virial expansion take the form

$$\frac{p_{\rm HS}}{nkT} = 1 + 4\eta + 10\eta^2 + 18.365\eta^3 + \cdots, \tag{29}$$

where the volume packing fraction η (the volume of the hard spheres divided by the total volume of the system) is given by $\eta = \frac{\pi}{6} n r_{\rm p}^3$. The *Carnahan-Starling* expression is a convenient and remarkably accurate fitting formula to this behaviour:

$$\frac{p_{\rm HS}}{nkT} = \frac{1 + \eta + \eta^2 - \eta^3}{(1-\eta)^3}. \tag{30}$$

The right hand side increases as the hard sphere packing fraction increases, and can be used to approximate the pressure at densities high enough to bring about the transition of the fluid to a

solid. From this we can construct the Helmholtz free energy using the relationship

$$F_{\rm HS} = F_{\rm ig} + NkT\frac{\eta\,(4-3\eta)}{(1-\eta)^2}. \tag{31}$$

This expression is conveniently verified by recovering Eq. (30) using

$$p_{\rm HS} = -\left(\frac{\partial F_{\rm HS}}{\partial V}\right)_{N,T}. \tag{32}$$

Thus

$$\begin{aligned} -\left(\frac{\partial F_{\rm HS}}{\partial V}\right)_{N,T} &= -\left(\frac{\partial}{\partial V}\right)_{N,T}\left[NkT\left(\ln[N/(Vn_q)]-1\right) + NkT\frac{\eta\,(4-3\eta)}{(1-\eta)^2}\right] \\ &= NkT/V - NkT\left(\frac{\partial}{\partial V}\right)_{N,T}\frac{\eta\,(4-3\eta)}{(1-\eta)^2}. \end{aligned} \tag{33}$$

The second term on the right hand side can be written

$$\frac{NkT}{V^2}\left(\frac{\partial}{\partial(1/V)}\right)_{N,T}\frac{\eta\,(4-3\eta)}{(1-\eta)^2} = \frac{N^2kT}{V^2}\left(\frac{\partial}{\partial(N/V)}\right)_{N,T}\frac{\eta\,(4-3\eta)}{(1-\eta)^2} = \frac{NkT\eta}{V}\left(\frac{\partial}{\partial\eta}\right)\frac{\eta\,(4-3\eta)}{(1-\eta)^2}, \tag{34}$$

and we get

$$p_{\rm HS} = \frac{NkT}{V} + \frac{NkT\eta}{V}\left[\frac{(1-\eta)}{(1-\eta)^3}(4-6\eta) + 2\frac{\eta(4-3\eta)}{(1-\eta)^3}\right] = \frac{NkT}{V} + \frac{NkT\eta}{V\,(1-\eta)^3}\left[4-10\eta+6\eta^2+8\eta-6\eta^2\right], \tag{35}$$

so

$$\frac{p_{\rm HS}}{nkT} = 1 + \frac{\eta}{(1-\eta)^3}\left[4-2\eta\right] = \frac{1-3\eta+3\eta^2-\eta^3+4\eta-2\eta^2}{(1-\eta)^3}, \tag{36}$$

which reduces to Eq. (30). The pressure is sketched in Figure 3 showing how it rises as the packing fraction increases.

We can take approximate account of the attractive long range tail of the interparticle interactions by adding the perturbative energy contribution $Vn^2\int_{r_{\rm p}}^{\infty} 2\pi r^2\phi(r){\rm d}r$ to the free energy, using Eq. (26), giving us

$$F_{\rm AHS} = NkT[\ln(n/n_q)-1] + NkT\frac{\eta\,(4-3\eta)}{(1-\eta)^2} - Van^2, \tag{37}$$

where $a = -\int_{r_{\rm p}}^{\infty} 2\pi r^2\phi(r){\rm d}r$, as before. We should also note that the packing fraction can be related to the van der Waals parameter b through $\eta = nb/4$.

The equation of state of the weakly attractive hard sphere fluid, obtained by taking the negative derivative with respect to V of the free energy in Eq. (37) is

$$p_{\rm AHS} = p_{\rm HS} - an^2. \tag{38}$$

The additional term is sufficient to bring about a phase change from gas to liquid, which we explore in the next section.

4 Phase coexistence

4.1 The availability potential

The simple model of a fluid discussed so far allows us to make a case for understanding phase coexistence, though more elaborate models will be needed for a successful matching of experimental data.

We begin by recalling from classical thermodynamics that the criterion for coexistence between two distinct phases of matter is that they should have equal chemical potentials and pressures. The Maxwell construction to identify coexisting dense and rarefied phases using the equation of state is typically employed. A more useful and intuitive point of view is to consider a system in contact with

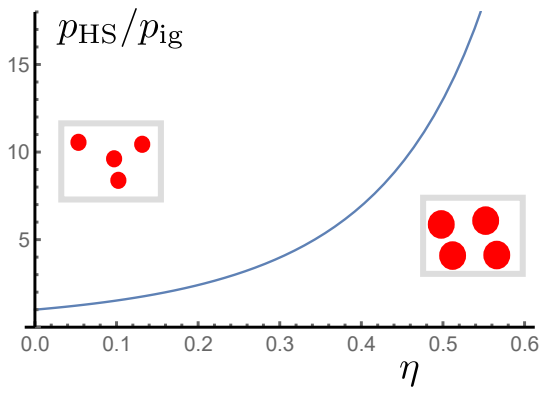

Figure 3: Hard sphere pressure, compared with the pressure of an ideal gas of point particles, as a function of packing fraction η, according to the Carnahan-Starling model.

heat and particle baths and to regard the phase selection rule in classical thermodynamics to be the minimisation of a thermodynamic potential, the availability function $\mathcal{A}$, with respect to density.

The availability is similar in form to the grand potential: for a large system, the minimised availability is indeed equal to the grand potential. For small systems, there is a more subtle connection between availability and grand potential. We define availability as

$$\mathcal{A}(N,V,T,\mu) = F(N,V,T) - \mu N. \tag{39}$$

The grand canonical partition function is then written as

$$Z_G(\mu,V,T) = \sum_{N=0}^{\infty} \exp\left(\mu N/kT\right) Z(N,V,T) = \sum_{N} \exp\left(-(F(N,V,T)-\mu N)/kT\right) = \sum_{N} \exp\left(-\mathcal{A}(N,V,T,\mu)/kT\right), \tag{40}$$

and the grand potential Φ, defined by $\Phi = -kT \ln Z_G$, is given by

$$\Phi(\mu,V,T) = -kT \ln \left[\sum_{N=0}^{\infty} \exp\left(-\mathcal{A}(N,V,T,\mu)/kT\right) \right]. \tag{41}$$

If one term $N = N_{\mathrm{m}}$ dominates the sum, such that $\mathcal{A}(N_{\mathrm{m}},V,T,\mu)$ is considerably smaller, in units of kT, than $\mathcal{A}(N,V,T,\mu)$ for $N \neq N_{\mathrm{m}}$, then we can see that $\Phi(\mu,V,T) \approx \mathcal{A}(N_{\mathrm{m}},V,T,\mu) = F(N_{\mathrm{m}},V,T) - \mu N_{\mathrm{m}}$. N_{m} is the (μ, V and T dependent) particle population that minimises the availability. In classical thermodynamics of an open system we would say that this population is selected (by virtue of the contact with the environmental particle bath) as a consequence of the second law of thermodynamics. The corrections to this approximation vanish for large systems, and the grand potential can be equated to the availability when minimised over N, as stated earlier. If the sum is not so dominated, then we must use Eq. (41) to specify Φ.

4.2 Availability of a weakly attractive hard sphere fluid

We shall demonstrate the use of the availability potential in understanding phase coexistence for a weakly attractive hard sphere fluid. We'll be able to characterise density fluctuations in the grand ensemble, going beyond our treatment of the ideal gas in section 2.

In order to provide a graphical approach, we shall employ an *excess* chemical potential with respect to a reference value $\mu_{\mathrm{ref}} = kT\ln(4/bn_q)$ and write $\mu = \mu_{\mathrm{ref}} + \mu_{\mathrm{ex}}$. Using Eq. (37) we then construct an availability function of a homogeneous fluid of N particles:

$$\mathcal{A}(N) = F_{\mathrm{AHS}} - \mu N = NkT[\ln(n/n_q) - 1] + NkT\frac{\eta\,(4-3\eta)}{(1-\eta)^2} - Van^2 - \mu N, \tag{42}$$

which in terms of packing fraction η, and in dimensionless form, is

$$\frac{\mathcal{A}b}{VkT} = -4\eta\left(\frac{\mu_{\mathrm{ex}}}{kT} - \ln\eta + 1\right) + \frac{4\eta^2\,(4-3\eta)}{(1-\eta)^2} - \frac{16a\eta^2}{bkT}. \tag{43}$$

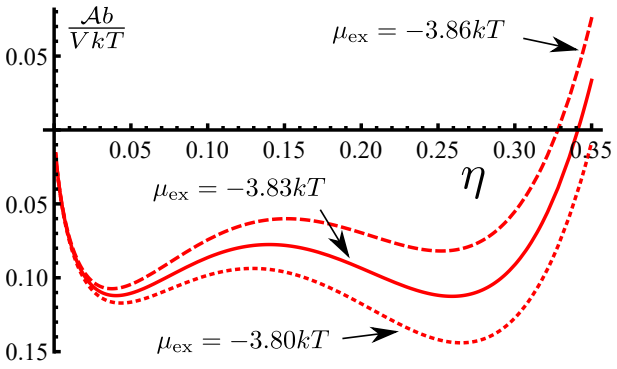

Figure 4: The minimum in the (dimensionless) availability function for the attractive hard sphere fluid identifies the macroscopic equilibrium system packing fraction for a given chemical potential represented in the form $\mu = kT\ln(4/bn_q) + \mu_{\rm ex}$. A phase transition accompanied by a discontinuity in density takes place as the excess chemical potential increases through the coexistence condition at $\mu_{\rm ex} = -3.83kT$. A value $a = 3bkT$ has been employed for illustration.

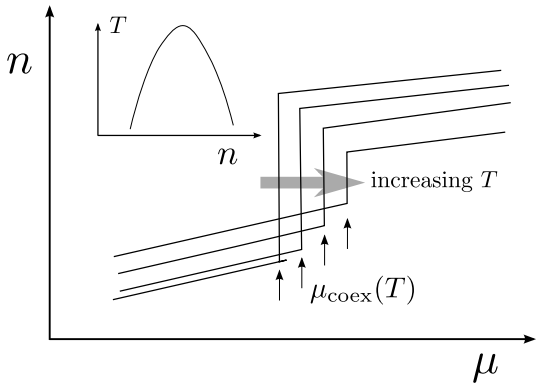

Figure 5: Sketch of fluid density as function of chemical potential for various temperatures (main plot); and of the densities of the coexisting phases (inset).

We plot this dimensionless availability as a function of packing fraction in Figure 4 for a specific value of the dimensionless combination $a/(bkT)$ and three values of $\mu_{\rm ex}/kT$. We confine our attentions here to a *large* system. Classical thermodynamics requires us to select the equilibrium phase (and its density) by identifying the global minimum of the availability. The double well shape gives rise to a condition of coexistence between a low and high density fluid (i.e. gas and liquid) at $\mu_{\rm ex}/kT \approx -3.83$ for $a = 3bkT$. For $\mu_{\rm ex}/kT \approx -3.8$ the liquid phase fills the system from the environmental particle bath but a reduction in environmental chemical potential corresponding to the more negative $\mu_{\rm ex}/kT \approx -3.86$ causes the density of material to fall, with a discontinuity at about -3.83.

A discontinuity in an *order parameter* (here the density), as sketched in Figure 5, is a hallmark of what are called *first order* phase transitions. More technically, such a transition is associated with a discontinuity in the slope of a plot of grand potential against chemical potential, but we need not go further into this matter. Second order phase transitions, which are rarer but have various points of interest, are associated with a discontinuity in the *second* derivative of a thermodynamic potential with respect to an environmental variable. In the present model, the discontinuity between the densities of the phases diminishes as the temperature rises until they merge at the so-called critical temperature, as shown in the inset to Figure 5.

5 Density fluctuations in a nonideal gas

Now we can use the free energy and availability potential of an attractive hard sphere fluid to understand how density fluctuations arise when a system is near a phase transition, or more generally when the system in question is *small* such that the mean particle population is low. Let us consider again the grand canonical ensemble probabilities of macrostates of the system defined by particle

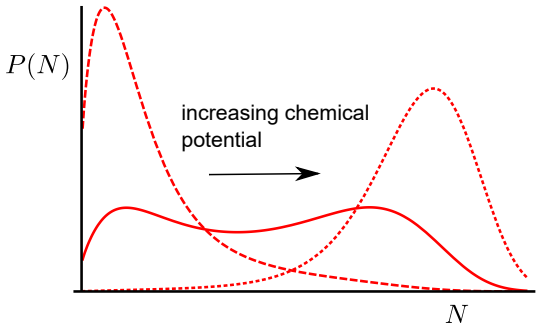

Figure 6: Equilibrium probability distributions describing density fluctuations in an open system: the system becomes bimodal as the chemical potential increases, corresponding to a phase transition. This sketch describes a small system where the peaks are fairly broad, suggesting that fluctuations are not negligible. The peaks become very narrow for large systems.

population. We have

$$P(N) = \frac{1}{Z_G}\exp(\mu N/kT)Z_N = \frac{1}{Z_G}\exp(-[F(N,V,T)-\mu N]/kT) = \exp([\Phi(\mu,V,T)-\mathcal{A}(N,V,T,\mu)]/kT), \tag{44}$$

and so an availability function with a double well shape as a function of N will give rise to a bimodal probability distribution in the equilibrium population. There will be peaks of probability of equal height at two values of N when the chemical potential of the system (and environment) is at the coexistence value for a given temperature.

For a large system where $\langle N\rangle$ is substantial for both phases, the peaks will be very narrow and the phase transition will be described by an abrupt shift in probability from one equilibrium density to the other as the chemical potential is moved through the coexistence point. For a small system, on the other hand, the probability distribution is broad and we would see a more gentle evolution in its shape as the chemical potential is changed. A sketch of the distribution $P(N)$ (represented here, for convenience, as a curve rather than as a set of discrete points) for three values of the chemical potential is shown in Figure 6. Away from coexistence conditions, we would expect to see fluctuations in system population about the mean values for the two equilibrium phases. At conditions close to coexistence we would also expect to see major fluctuations in population as a consequence of the bimodality of the pdf in such an environment. The situation may be contrasted with the density fluctuations of an ideal gas considered in Eq. (8) and Figure 1. The differences are brought about by the interactions between particles that stabilise larger fluctuations.

We shall come to see that in sufficiently small systems, such population fluctuations correspond to the formation of clusters of particles, at least for the gas-liquid phase transition under consideration here. By constructing a free energy function $F(N,T)$, or equivalently a canonical partition function that represents a single cluster in the system, it is possible to build a model of the formation, or *nucleation*, of a macroscopic droplet from the vapour. We shall be able to interpret the peak in the availability function as a thermodynamic barrier controlling the nucleation of droplets of stable condensed phase starting from a metastable gaseous phase.

It should be recognised that many phase transitions, not just that between a gaseous and condensed phase, can be described by similar statistical mechanical approaches. In general, the phases involved in the transition are characterised by an *order parameter*: in the above we used the particle density. In the transformation from a liquid to a solid, the order parameter is in part the density, but more importantly the emerging discrete translational symmetry in the arrangement of particles. For phase transitions in magnets, the order parameter might be the strength of the magnetisation. In the phase transition from a normal metal to a superconductor, the order parameter is related to the proportion of electrons that have entered a state of Bose-Einstein condensation. In each case, the system (if it is large enough) seeks equilibrium through the minimisation of an availability potential with respect to an order parameter. In doing so, the system is following the imperative of the second law of thermodynamics. If the system is small, then fluctuations are more apparent, but they are again characterised by the availability function.

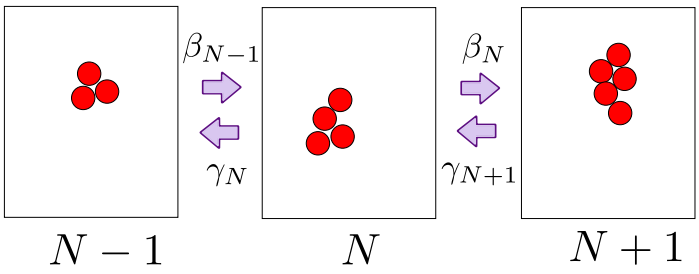

Figure 7: Transitions between system macrostates labelled by particle number N, and illustrated by snapshots of molecular clusters. Growth and evaporation processes take place according to transition probabilities per unit time β_N and γ_N, respectively.

6 Cluster dynamics and droplet nucleation

We now use the ideas of *macrostate probability dynamics* in the context of density fluctuations in a nonideal gas. Our aim is to develop models of the *nucleation* of condensed phase droplets from a *metastable* vapour, namely one that is placed under conditions outside the normal gaseous region of the phase diagram. It is possible, with care, to cool a vapour below its so-called dew point, or compressed to make its pressure exceed the saturated vapour pressure. We want to understand how the phase transition develops and to compute the rate of droplet formation, or equivalently the time that a phase can be maintained in a metastable state.

In order to do this we need to define a set of macrostates and the transition probabilities between them, and then construct a set of *master equations* governing the occupational probabilities and solve them. The equilibrium grand canonical probability distribution over the macrostate phase space of cluster size is a reference case that will help us define the probability dynamics.

6.1 Becker-Döring equations

If the system volume has spatial dimensions of the order of nanometres, the principal microstates in the phase space will consist of a single molecular cluster, bound together by interparticle attractive forces. Snapshots of such clusters are shown in Figure 7. The clusters will define our macrostates and will be labelled by the number of particles N within them. The neglected details of the environmental dynamics are represented through transition probabilities for changes in the number of particles in the system, representing the effects of agglomeration between the cluster in the system and a monomer from the environment, or the evaporative loss of a monomer from the cluster to the environment. The gain or loss of a molecular dimer, or even bigger clusters, is assumed to be rare. This physical motivation helps us to construct a set of master equations for the probabilities $P_N(t)$ that the system should contain an N-cluster:

$$\frac{\mathrm{d}P_N}{\mathrm{d}t} = \beta_{N-1}P_{N-1} - \gamma_N P_N - \beta_N P_N + \gamma_{N+1}P_{N+1}, \tag{45}$$

where β_N and γ_N are transition probabilities, per unit time, that an N-cluster macrostate should gain or lose a particle, respectively. We expect that these transition rates might depend on the condition of the environment, namely its chemical potential and temperature. The above are known as the *Becker-Döring equations* and they describe a so-called *birth/death* process.

The master equations can be expressed in terms of a current $j_N = \beta_N P_N - \gamma_{N+1}P_{N+1}$ describing the flow of probability between macrostates N and $N+1$. We can write $\mathrm{d}P_N/\mathrm{d}t = j_{N-1} - j_N$ and furthermore, we can identify a condition of *detailed balance* for zero probability current:

$$\beta_N P_N^{\mathrm{eq}} = \gamma_{N+1}P_{N+1}^{\mathrm{eq}}, \tag{46}$$

where we have introduced probabilities P_N^{eq} describing a state of equilibrium (grand canonical in this case) between the system and its environment.

We know from our earlier discussion of density fluctuations and Eq. (44) that the equilibrium macrostate probabilities are given by $P_N^{\mathrm{eq}} \propto \exp(-[F(N) - \mu N]/kT) = \exp(-\mathcal{A}(N)/kT)$ where $F(N)$ is the free energy of the system (here an N-cluster) and $\mathcal{A}(N)$ is its availability potential in the given environment. The free energy and hence the availability will depend on the system volume

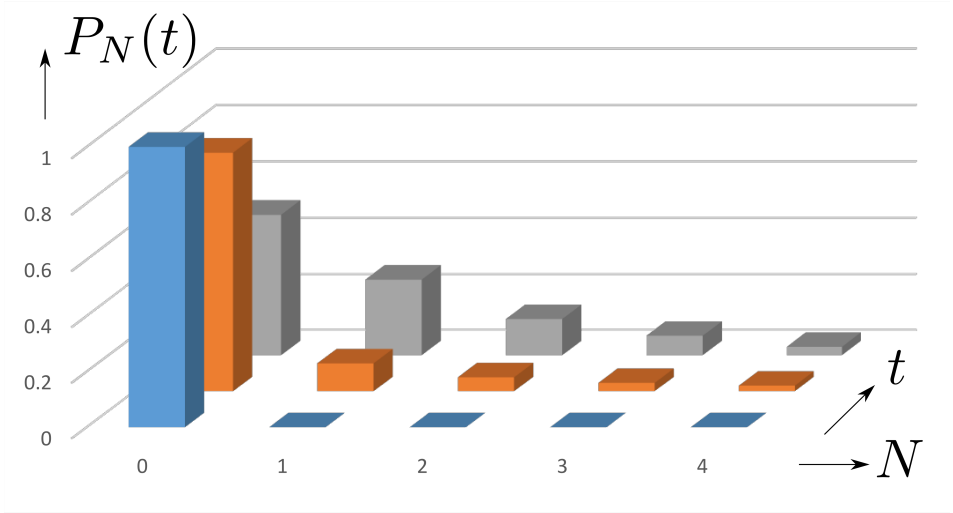

Figure 8: Illustration of the solution to a master equation describing the relaxation to equilibrium of probabilities $P_N(t)$ for the presence of an N particle cluster inside a system coupled to an environment.

as well as particle content, but we suppress this notationally. The gain and loss (or growth and decay) transition rate coefficients must satisfy

$$\frac{\gamma_{N+1}}{\beta_N} = \frac{P_N^{\rm eq}}{P_{N+1}^{\rm eq}} = \exp([\mathcal{A}(N+1) - \mathcal{A}(N)]/kT). \tag{47}$$

The next step is to assert on physical grounds that the probability per unit time of cluster growth β_N is proportional to a (presumed) monomer density n_1 in the environment. This is how the monomer-cluster collision rate would scale. If we regard the environment as an ideal gas, then this density is related to its chemical potential according to $\mu = kT\ln(n_1/n_q)$, so $\beta_N \propto \exp(\mu/kT)$. We write $\beta_N = \beta_0 \exp(\mu/kT)$ where, according to kinetic theory, β_0 would correspond to an approach velocity multiplied by a capture cross section, together with other factors. We then can write

$$\gamma_{N+1} = \beta_0 \exp([F(N+1) - F(N)]/kT), \tag{48}$$

and hence we have a full specification of the transition coefficients in the Becker-Döring equations in terms of the free energies of the N-cluster macrostates (and hence their canonical partition functions) and the chemical potential (or equivalently the monomer density) of the surrounding vapour. Thus we can model the nonequilibrium evolution of the macrostate probabilities P_N towards the equilibrium distribution $P_N^{\rm eq}$, starting from an arbitrary initial condition.

As an example, consider an initial situation $P_0(0) = 1$ with $P_N(0) = 0$ for $N > 1$, which states that we are certain that the system is initially empty of particles. In order to model the nonequilibrium statistical mechanics of the change in population (cluster size) with time, we would solve the Becker-Döring equations and observe the spreading out of the initial probability spike at $N = 0$ to form a time independent equilibrium distribution, as illustrated in Figure 8 (in this case for a $P_N^{\rm eq}$ that monotonically decreases with N). We could use the evolving $P_N(t)$ to compute expectation values, such as $\langle N\rangle_t = \sum_0^\infty N\, P_N(t)$, the mean size of the cluster, and hence we could describe the relaxation towards a statistical state of equilibrium.

6.2 Nucleation barrier and critical size

The probability dynamics become more interesting if we consider a relaxation from an initial state towards an equilibrium probability distribution $P_N^{\rm eq}$ that is *bimodal*. There will be a cluster size range between the modes that has low probability at equilibrium, and which acts as a bottleneck for the flow of probability current. It turns out that if the initial distribution of probability lies principally on one side of this region, there will be a period during the subsequent relaxation when the probability passes relatively slowly from one mode into the other. This is illustrated in Figure 9, using continuous, instead of discrete, initial and equilibrium pdfs for clarity. The equilibrium distribution will be related to a double well profile of the availability, as was discussed in section

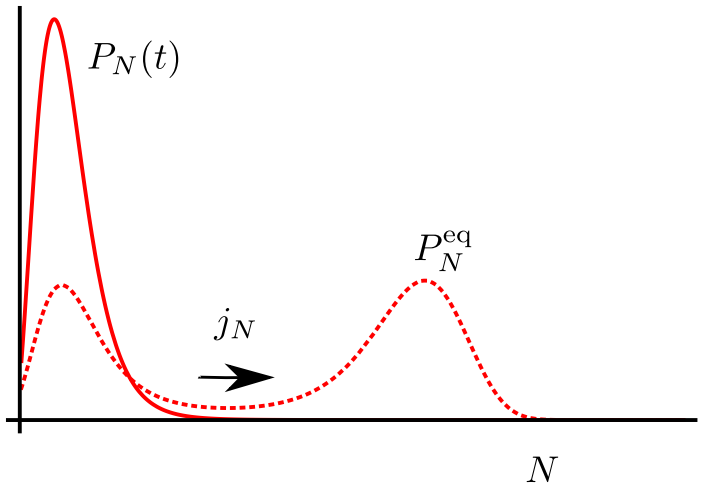

Figure 9: The evolution of a probability distribution from a nonequilibrium initial state towards a bimodal equilibrium profile $P_N^{\rm eq}$. The bottleneck in the process is the rate at which probability can pass across the central region in the phase space, which is described by a current j_N.

4. We shall interpret the draining of probability between modes as the overcoming of a barrier represented by this thermodynamic potential: a *nucleation* event.

It will turn out to be convenient to write the cluster free energy as

$$F(N,V,T) = N\mu_{\rm coex} + F_{\rm exc}(N,T) + f(V), \tag{49}$$

where $F_{\rm exc}$ is called the *excess* free energy and $\mu_{\rm coex}$ is the chemical potential at which there is coexistence between the bulk vapour and condensed phases (see Section 4). The final term carries the volume dependence of F and can be neglected since it will cancel out in all physical situations. In classical thermodynamics we would expect a free energy to be extensive, that is proportional to the number of particles in the system. But for small clusters, we are far from the thermodynamic limit and the excess free energy need not be proportional to N.

We can write the availability of a cluster as

$$\mathcal{A}(N) = F(N) - \mu N = F_{\rm exc}(N) - N\Delta\mu, \tag{50}$$

where $\Delta\mu = \mu - \mu_{\rm coex}$. From our earlier discussions of phase stability in Section 4, if $\mu > \mu_{\rm coex}$ we expect to find that the global minimum in the availability potential should lie at large N, reflecting the thermodynamic stability of the condensed phase. If $\Delta\mu < 0$ then the global minimum should most likely reside at $N = 0$, corresponding to the (rarefied) vapour.

The excess free energy is a property of the cluster, computable from the partition function. It typically increases sublinearly with N (for example $F_{\rm exc} \propto N^{2/3}$) and we shall focus on such a situation here. A toy availability function $\mathcal{A}(N) = \theta N^{2/3} - N\Delta\mu$, with positive constant θ and positive $\Delta\mu$, rises at first for small cluster sizes, reaches a peak and then decreases. This situation is shown in Figure 10: the existence of a deep well further out on the right hand side is implied. The ratio of evaporation to growth parameters in the master equations, $\gamma_{N+1}/\beta_N = \exp[(\mathcal{A}(N+1) - \mathcal{A}(N))/kT]$, consistent with this availability function is also shown.

The availability goes through a maximum equal to $\mathcal{A}^*$ at a so-called *critical size* N^*. For cluster sizes smaller than the critical size, the rate of loss of a particle (by evaporation) is greater than the rate of particle gain (by agglomeration), while for sizes above this threshold, the situation is reversed, as demonstrated by the plotted ratio γ_{N+1}/β_N. There is clearly a pattern of a preference for clusters to evaporate at small sizes that develops into an inclination to grow at large sizes. This allows us to visualise the formation of condensed phase droplets from a metastable vapour phase as the crossing of a bottleneck region in cluster size space, or the surmounting of an availability potential barrier, brought about by thermal fluctuation.

6.3 Solution to the rate equations

The nucleation process can be investigated by solving the Becker-Döring equations subject to boundary conditions on the probability profile such that a steady probability current is produced. We solve for a stationary nonzero current $j_N = j$:

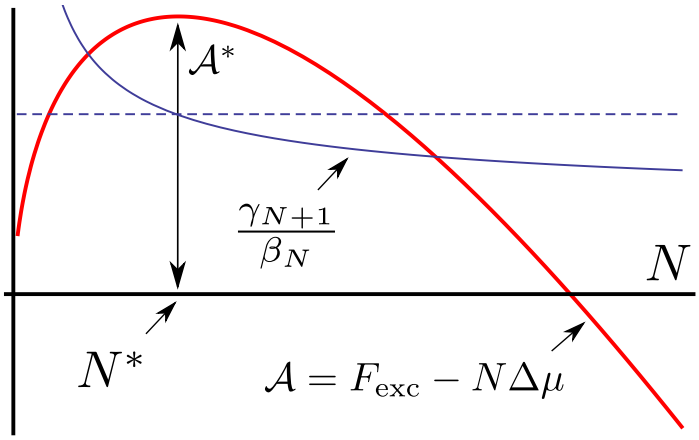

Figure 10: The red curve is the availability $\mathcal{A}(N)$ controlling the process of nucleation by processes of molecular cluster growth and evaporation (shown for clarity as a continuous line). The profile corresponds to a set of rate coefficients β_N and γ_N in the Becker-Döring equations. For clusters smaller than the critical size N^*, transitions that decrease cluster size N are more likely than transitions that increase N. The ratio γ_{N+1}/β_N passes through unity (the dashed line) at the critical size, and then the relative magnitude of the transition probabilities reverses. The height of the availability barrier $\mathcal{A}^*$ controls the stationary nucleation rate of droplets arising from a metastable vapour.

$$j = \beta_N P_N - \gamma_{N+1} P_{N+1}, \tag{51}$$

having set the probability that a monomer P_1 should occupy the system to be a constant, and the probability $P_{N_{\rm max}}$ for a cluster at a size $N_{\rm max}$ to be zero. These conditions are simplifications of the idea that the macrostate dynamics evolve a cluster from a monomer through the stochastic processes of growth and evaporation, and as soon as the cluster reaches a certain size $N_{\rm max}$ it is removed and we start again with a fresh monomer.

We shall cast these equations in a slightly different form, where the probabilities for the presence of a single cluster in a small system volume are replaced by the *mean population densities* of clusters n_N in a large system. The master equations then become

$$J = \beta_N n_N - \gamma_{N+1} n_{N+1}, \tag{52}$$

which are usually called *rate equations*, and the current J is now the rate of passage of clusters between sizes N and $N+1$, per unit time and volume of vapour: the droplet *nucleation rate*.

The solution to the Becker-Döring rate equations is obtained by a straightforward but lengthy elimination procedure. We write

$$\begin{aligned} J &= \beta_1 n_1 - \gamma_2 n_2 \\ J &= \beta_2 n_2 - \gamma_3 n_3 \\ &\cdots \\ J &= \beta_{N_{\rm max}-1} n_{N_{\rm max}-1} - \gamma_{N_{\rm max}} n_{N_{\rm max}}, \end{aligned} \tag{53}$$

and solve for the n_2, n_3, etc, subject to boundary conditions $n_1 = \text{const}$ and $n_{N_{\rm max}} = 0$. We define $\alpha_k = \gamma_k/\beta_k$ and multiply the left hand side of the $i^{\rm th}$ equation by a product $\prod_{k=2}^{i} \alpha_k$. The first three equations are then

$$\begin{aligned} J &= \beta_1 n_1 - \gamma_2 n_2 \\ \prod_{k=2}^{2} \alpha_k J &= \prod_{k=2}^{2} \alpha_k \beta_2 n_2 - \prod_{k=2}^{2} \alpha_k \gamma_3 n_3 = \gamma_2 n_2 - \prod_{k=2}^{2} \alpha_k \gamma_3 n_3 \\ \prod_{k=2}^{3} \alpha_k J &= \prod_{k=2}^{3} \alpha_k \beta_3 n_3 - \prod_{k=2}^{3} \alpha_k \gamma_4 n_4 = \prod_{k=2}^{2} \alpha_k \gamma_3 n_3 - \prod_{k=2}^{3} \alpha_k \gamma_4 n_4. \end{aligned} \tag{54}$$

The key thing to notice is that when we add all the equations together, there will be repeated cancellation between terms on the right hand sides. The last two equations are

$$\begin{aligned}
\prod_{k=2}^{N_{\max}-2} \alpha_k J &= \prod_{k=2}^{N_{\max}-2} \alpha_k \beta_{N_{\max}-2} n_{N_{\max}-2} - \prod_{k=2}^{N_{\max}-2} \alpha_k \gamma_{N_{\max}-1} n_{N_{\max}-1} \\
&= \prod_{k=2}^{N_{\max}-3} \alpha_k \gamma_{N_{\max}-2} n_{N_{\max}-2} - \prod_{k=2}^{N_{\max}-2} \alpha_k \gamma_{N_{\max}-1} n_{N_{\max}-1} \\
\prod_{k=2}^{N_{\max}-1} \alpha_k J &= \prod_{k=2}^{N_{\max}-1} \alpha_k \beta_{N_{\max}-1} n_{N_{\max}-1} = \prod_{k=2}^{N_{\max}-2} \alpha_k \gamma_{N_{\max}-1} n_{N_{\max}-1},
\end{aligned} \tag{55}$$

which exhibits the same pattern. The sum of all the equations is then

$$J\left(1 + \sum_{N=2}^{N_{\max}-1} \prod_{k=2}^{N} \alpha_k\right) = \beta_1 n_1. \tag{56}$$

Next we note that

$$\prod_{k=2}^{N} \alpha_k = \prod_{k=2}^{N} \frac{\gamma_k}{\beta_k} = \frac{\beta_1}{\beta_N} \prod_{k=2}^{N} \frac{\gamma_k}{\beta_{k-1}} = \frac{\beta_1}{\beta_N} \prod_{k=2}^{N} \exp([\mathcal{A}(k)-\mathcal{A}(k-1)]/kT) = \frac{\beta_1}{\beta_N} \exp([\mathcal{A}(N)-\mathcal{A}(1)]/kT), \tag{57}$$

so we can write

$$J = \frac{\beta_1 n_1}{1 + \sum_{N=2}^{N_{\max}-1} \frac{\beta_1}{\beta_N} \exp([\mathcal{A}(N) - \mathcal{A}(1)]/kT)}, \tag{58}$$

which is the exact nucleation rate in terms of the cluster availability function, the monomer population and the rate coefficients β_N. Note that it is a *difference* in availability potential that controls the rate: the irrelevance of a volume-dependent term $f(V)$ in the free energy in Eq. (49) is now demonstrated.

A rough simplification of this expression is obtained by approximating the denominator by the largest term in the sum, the one that has the maximum value of $\mathcal{A}(N)$. This also identifies N^*, the critical size. In passing, it should be noted that as long as the maximum size $N_{\max}$, introduced to terminate our set of equations, is rather larger than N^*, its actual value is immaterial. The nucleation rate can then be written in the approximate form

$$J \approx \frac{\beta_{N^*} n_1}{\exp([\mathcal{A}(N^*) - \mathcal{A}(1)]/kT)} \propto n_1^2 \exp(-[\mathcal{A}(N^*) - \mathcal{A}(1)]/kT), \tag{59}$$

since the growth rates β_N are proportional to the monomer population, as previously noted.

The proportionality to the square of the monomer density is a reminder that nucleation is driven by collisions, but the most important message to grasp from this result is that the nucleation rate is controlled by the maximum availability $\mathcal{A}(N^*) = \mathcal{A}^*$, shown in Figure 10. The expression and the analysis provides a mathematical underpinning of a general rule in statistical physics, and in chemistry, that the rate of crossing of a thermodynamic barrier is proportional to the exponential of the negative of the barrier height; a Boltzmann factor.

In the context of modelling the nucleation process, it is traditional to define a quantity that we shall call the nucleation barrier potential:

$$\Delta\phi(N) = \mathcal{A}(N) - \mathcal{A}(1) = \Delta F_{\rm exc}(N) - (N-1)\Delta\mu, \tag{60}$$

where $\Delta\mu = \mu - \mu_{\rm coex}$, and $\Delta F_{\rm exc}(N) = F_{\rm exc}(N) - F_{\rm exc}(1)$, a difference between the excess free energy $F_{\rm exc}(N)$ of a cluster of size N, defined in Eq. (5), and the excess free energy of a monomer. Fundamentally, $\Delta F_{\rm exc}$ is to be computed from the canonical partition function of a cluster, for which various methods have been developed but will not be discussed here.

The $\Delta F_{\rm exc}(N)$ term in Eq. (60) typically turns out to increase sublinearly in N while the second decreases linearly, for positive $\Delta\mu$ corresponding to conditions favouring condensation in the system. The contributions give rise to a barrier, as illustrated in Figure 10, that the cluster has to surmount if it is to nucleate into a large droplet. If the excess free energy were zero, then $\Delta\phi(N)$ would be linear in N and there would be no barrier. This makes $\Delta F_{\rm exc}$ the focus of attention in nucleation theory and explains why it makes sense to introduce it through Eq. (49).

If we treat N as a continuous variable, then the critical size N^*, where $\Delta\phi(N)$ is at a maximum, may be found from the condition

$$\frac{\mathrm{d}\Delta\phi}{\mathrm{d}N} = \frac{\mathrm{d}\Delta F_{\mathrm{exc}}}{\mathrm{d}N} - \Delta\mu = 0, \tag{61}$$

and the nucleation rate J would be proportional to a Boltzmann factor corresponding to the height of the barrier,

$$J \approx \beta_{N^*} n_1 \exp(-\Delta\phi(N^*)/kT). \tag{62}$$

.

6.4 Classical nucleation theory

A very widely used model of cluster thermodynamics asserts that the principal contribution to the excess free energy ΔF_{exc} of an N-cluster is a term proportional to its notional *surface area*. The model is based on the idea that a cluster resembles a spherical droplet with the interior density of the bulk condensate (a phase that has a free energy approximated by μ_{coex} per particle) and the surface tension σ of a macroscopic condensed phase. These assumptions are known as the *capillarity approximation*. Such assumed geometry, density and surface properties are only really appropriate for clusters with very large values of N, and we would not expect this approach to be an accurate model for clusters of only a few molecules.

Specifically we would write

$$\Delta F_{\mathrm{exc}}(N) \approx 4\pi R_N^2 \sigma, \tag{63}$$

where R_N is the droplet radius and $4\pi R_N^2$ its surface area. The surface tension corresponds to a free energy per unit area. Why is this? Recall that surface tension is *defined* through the fundamental relation of thermodynamics $\mathrm{d}E = T\mathrm{d}S - p\mathrm{d}V + \mu\mathrm{d}N + \sigma\mathrm{d}A$, where $\mathrm{d}A$ is an increment in system surface area. Thus $\mathrm{d}F = -S\mathrm{d}T - p\mathrm{d}V + \mu\mathrm{d}N + \sigma\mathrm{d}A$ and so $\sigma = (\partial F/\partial A)_{T,V,N}$.

The droplet radius may be written

$$R_N = \left(\frac{3N}{4\pi n_\ell}\right)^{1/3}, \tag{64}$$

where n_ℓ is the particle density in the bulk condensed (liquid) phase, such that

$$\Delta F_{\mathrm{exc}}(N) = 4\pi\sigma \left(\frac{3N}{4\pi n_\ell}\right)^{2/3} = \theta N^{2/3}, \tag{65}$$

where $\theta = (6\pi^{1/2}/n_\ell)^{2/3}\sigma$ is a coefficient that depends on the physical properties n_ℓ and σ. This expression for $\Delta F_{\mathrm{exc}}(N)$ does not vanish at $N = 1$ as it should, but in classical theory we assume that the relevant critical cluster size is large, so it is only meant to be appropriate for large N.

Then we solve Eq. (61) to obtain the critical cluster size:

$$\frac{2}{3}\theta N^{-1/3} - \Delta\mu = 0 \qquad \Rightarrow N^* = \left(\frac{2\theta}{3\Delta\mu}\right)^3, \tag{66}$$

which leads to a height of the nucleation barrier:

$$\Delta\phi(N^*) = \theta N^{*2/3} - (N^*-1)\Delta\mu = \theta\left(\frac{2\theta}{3\Delta\mu}\right)^2 - \left(\frac{2\theta}{3\Delta\mu}\right)^3\Delta\mu + \Delta\mu = \frac{\theta}{3}\left(\frac{2\theta}{3\Delta\mu}\right)^2 + \Delta\mu = \frac{4\theta^3}{27(\Delta\mu)^2} + \Delta\mu. \tag{67}$$

Note that we can write

$$\Delta\mu = \mu - \mu_{\mathrm{coex}} = kT\ln(n_1/n_1^{\mathrm{sat}}), \tag{68}$$

through representing the chemical potential using the ideal gas expression, Eq. (4), and introducing a monomer density $n_1^{\mathrm{sat}}(T)$ appropriate to a *saturated* vapour, namely a gas phase that is in coexistence with the condensed phase at the temperature of the environment. The ratio of the monomer density in a metastable vapour to its value in a saturated vapour is called the supersaturation, $\mathcal{S}$, (not to be confused with entropy!), also referred to as the relative humidity in the case of water, and so we can write $\Delta\mu = kT\ln\mathcal{S}$. The classical nucleation rate of droplets can then be obtained by combining Eqs. (62), (67) and (68):

$$J_{\mathrm{CNT}} \approx \beta_{N^*} n_1^{\mathrm{sat}} \exp\left(-\frac{4\theta^3}{27(kT)^3(\ln\mathcal{S})^2}\right). \tag{69}$$

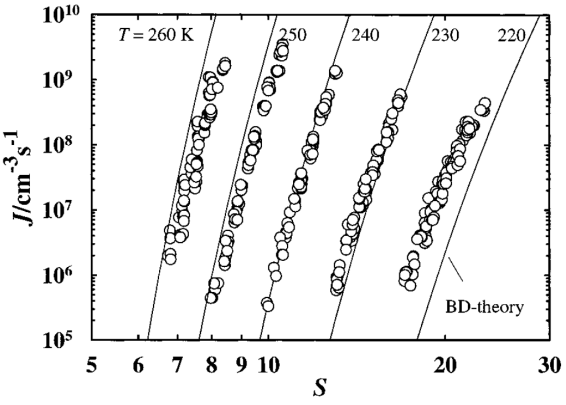

Figure 11: Experimental values of nucleation rate of water droplets (circles) under a range of conditions of temperature T and vapour supersaturation $\mathcal{S}$, compared with the predictions of classical nucleation theory, Eq. (69), labelled 'BD-theory'.

The classical nucleation rate does account roughly for the experimentally measured rates of formation of droplets from some metastable vapours, and extensions have been added to allow it to be applied to the freezing of liquids and the crystallisation of solutes from solvents. Putting physical data and typical experimental conditions into Eq. (66) gives critical sizes of a few tens of molecules and heights of the nucleation barrier of a few tens of kT.

We can illustrate this for water vapour under conditions studied experimentally. We shall use $\sigma \approx 0.077$ N/m, $n_\ell \approx 3.34 \times 10^{28}$ m^{-3} such that $\theta \approx 3.62 \times 10^{-20}$ J. For $T = 260$ K and $\mathcal{S} = 7.2$ (i.e. 720% relative humidity) we would predict a critical cluster size of $N^* \approx 39$, a critical cluster radius of $R^* = 0.66$ nm and nucleation barrier height of about $39\,kT$. The rate of monomer attachment to the critical cluster β_{N^*} can be regarded as the product of the critical cluster surface area and the molecular flux in the vapour. This can be estimated to be $4\pi R^{*2} n_1^{\rm sat} \bar{v}$, where $\bar{v}$ is the molecular root mean square velocity. Using a saturated vapour monomer density of $n_1^{\rm sat} \approx 6.19 \times 10^{22}$ m^{-3}, for $T = 260$ K, and $\bar{v} \approx \sqrt{kT/m} \sim 350$ ms^{-1}, where m is the molecular mass of water, we find that $\beta_{N^*} \approx 1.2 \times 10^8$ s^{-1} and we finally obtain a nucleation rate of $J \approx 10^8$ cm^{-3}s^{-1}. This would make a very dense mist of very fine nanoparticles! Bear in mind that the supersaturation and temperature are deliberately chosen in the experiment to produce a high rate of droplet formation.

Figure 11 is a comparison between the predictions of classical nucleation theory and experimental nucleation rates for water for a range of temperatures and vapour supersaturations, obtained in a small cloud chamber and published by Wölk *et al* (J. Phys. Chem. B105, 11685 (2001)). The reasonable agreement is remarkable, considering the approximations made in the droplet model.

Classical nucleation theory is not always successful, however, primarily because the capillarity approximation upon which it is based is a very primitive characterisation of small molecular clusters. Nevertheless, the expression in (69) has intuitive value in that it suggests that in order to drive the nucleation of droplets at a faster rate, we need to increase the vapour supersaturation $\mathcal{S}$, all other parameters being held constant. Also, the nucleation rate depends on the surface tension of the condensed phase: the higher the surface tension σ, and hence θ, the slower the rate. The other lesson is that the rate is rather sensitive to supersaturation, surface tension and temperature since these quantities appear inside an exponential.

To do better than classical theory, it is necessary to compute the partition functions of clusters of various sizes and develop a more realistic model of the excess free energy, but this is beyond the scope of these lectures. However, as an illustration of what can be done, Figure 12 illustrates the excess free energy of water (modelled using the TIP4P(2005) intermolecular force field) obtained by Lau *et al* (J. Chem. Phys. 143, 244709 (2015)) using a method of steered molecular dynamics similar in effect to thermodynamic integration. Remarkably, the capillarity approximation seems to hold for clusters as small as a few tens of molecules, at least for this temperature and substance.

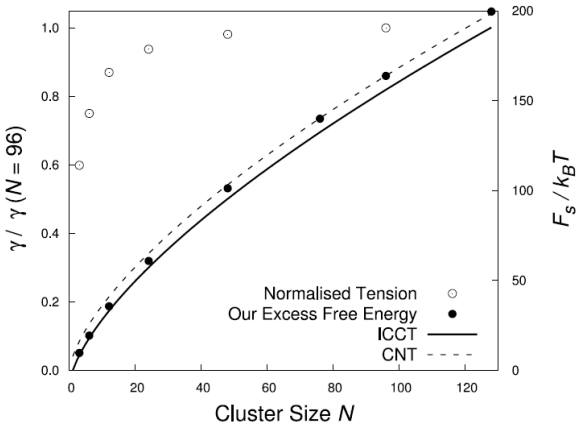

Figure 12: Excess free energy (here labelled F_s), right hand axis) for clusters of TIP4P(2005) water at 300 K, compared with the capillarity approximation (CNT) and a shifted version (ICCT). An effective surface tension (here labelled γ) as a function of cluster size is also shown (left hand axis).

7 Nucleation and the second law

If the nucleation process involves the need for a system to overcome an availability barrier, we should ask ourselves whether this is compatible with the second law. After all, we have been led to believe that Nature will seek to move a system *down* the gradient of availability, towards a minimum. When a nucleation event takes place, is it by virtue of a temporary negative fluctuation in the total entropy of the world? Does nucleation break the second law?

The answer to this question has only recently emerged through an application of the methods of *stochastic thermodynamics*. This framework has allowed a more general view of entropy and its production to be developed, one that is appropriate for the description of small systems and capable of accommodating thermal fluctuations. It is a valuable viewpoint since entropy production may be linked directly to the stochastic dynamics of a system: a random path taken by a cluster as it changes its size, under the influence of its environment, can be used to define a random path in the evolution of the total entropy of the world. The details are too many to discuss here, but the key result to consider is that the total *stochastic* entropy of the world changes with time according to the expression

$$\Delta s_{\rm tot} = \Delta s_{\rm sys} + \Delta s_{\rm env}, \tag{70}$$

namely as a sum of the change $\Delta s_{\rm sys}$ in a stochastic system entropy $s_{\rm sys}(N,t) = -k \ln p(N,t)$, and a change in a stochastic environmental entropy $\Delta s_{\rm env}$. Here, the system is described by a variable N and a probability distribution over its values p. The change in stochastic environmental entropy $\Delta s_{\rm env}$ for the case of a nucleating cluster is the negative change in its availability potential, divided by temperature. When a fluctuation takes a cluster over the nucleation barrier, the temporary increase in availability therefore produces a decrease (albeit fleeting) in the stochastic environmental entropy. This is the puzzle referred to in the first paragraph of this section: does this not imply a temporary breakage of the second law? But the resolution is that the change in stochastic system entropy needs also to be considered. The probability that a cluster is to be found near the top of the barrier is small, so when it finally does make it, the stochastic system entropy becomes large (small p implies large $s_{\rm sys}$) and it turns out that this outweighs the negative change in stochastic environmental entropy. As is so often found to be the case in thermodynamics, while parts of the world might see a reduction in entropy as a result of some process, this is compensated by a greater increase somewhere else, and the second law is respected.

What has not been mentioned here is that the framework of stochastic thermodynamics does in fact allow negative fluctuations in total stochastic entropy, but these are expected to emerge universally, and are not a consequence of barrier hopping. The second law in this framework states that such fluctuations in total entropy production satisfy what are called fluctuation relations, and that upon averaging over all possible dynamical evolutions, the total stochastic entropy of the world is *expected* to increase. Fluctuations are accommodated.

The formulation of total stochastic entropy production in Eq. (70) together with the second law embodied in the inequality $\langle \Delta s_{\rm tot} \rangle \geq 0$ constitute our best current understanding of the production of entropy in dynamic and thermodynamic models of open system behaviour.